Gain-Narrowed Light Emission from Self-organized Organic Microdots

Hisao Yanagi*

PRESTO, Japan Science and Technology Corporation (JST), Faculty of Engineering, Kobe University, Rokkodai, Nada-ku, Kobe 657-8501, Japan

Masatoshi Kondo and Naoki Matsuoka

Faculty of Engineering, Kobe University, Rokkodai, Nada-ku, Kobe 657-8501, Japan

Michifumi Nagawa and Yoshio Taniguchi

Faculty of Textile Science and Technology, Shinshu University, Ueda, Nagano 386-8567, Japan

Received July 17, 2001. Revised Manuscript Received August 28, 2001

Organic microdots were self-organized by vapor deposition of emissive distyrylbenzene derivative molecules onto a cleaved surface of a KCl single crystal. When the deposition amounts were changed at an elevated substrate temperature, the microdot diameters were controlled from the submicrometer scale up to larger than 10 μm. Under optical pumping using a pulse laser, the microdots encapsulated in an MgF_2 layer exhibited amplified spontaneous emission depending on the microdot size. While the spontaneous fluorescence band of the microdots smaller than the cutoff diameter of around 8 μm never collapsed even at high excitation energy, those beyond this size exhibited a gain-narrowed emission peak above a certain threshold energy.

Introduction

Organic electroluminescence (EL) devices[1,2] have just begun finding practical use as a full-color flat-panel display and further application to organic semiconductor lasers.[3] Schön et al. have recently demonstrated amplified spontaneous emission (ASE) and lasing in organic single crystals of tetracene[4] and α-sexithiophene[5] using field-effect electrodes. The first success of this organic solid-state injection laser is attributed to gate-controlled charge carrier injection at high density and mobility. The lack of defects in such high-quality single crystals can minimize the extrinsic effects of reduced luminescence efficiency.

On the other hand, disordered multilayer structures in organic EL devices using amorphous or polycrystalline thin films cause considerable exciton quenching by carrier trapping and nonradiative recombination at grain boundaries and interfaces, resulting in transitional degradation of light-emitting performances. To overcome the instability of organic materials under excitation with high current injection for lasing, further considerations have to be given to devise engineering for improving light amplification. In view of well-organized epitaxial layer structures and quantum structures in semiconductor light-emitting diodes (LEDs) and laser diodes (LDs), it is important to introduce an ordered structure in organic materials for efficient confinement of excitons and light. As pointed out by Schön et al.,[4] improvement of cavity or resonator structures should be considered for further reduction of the threshold current density to realize room-temperature organic LDs.

Incorporation of such amplifying structures have been demonstrated in distributed Bragg reflectors (DBRs),[6] distributed feedback (DFB),[7,8] microdiscs,[9] and so forth. Moreover, mesoscopic structures with a dielectric periodicity of dimension comparable to the wavelength of light have attracted interest as photonic crystals.[10−12] The radiative properties of photonic-crystal materials can be controlled by the concept of a photonic band gap. Most of such mesostructures of submicrometer scale have been prepared by chemical etching, patterned growth, and lithography of inorganic semiconductors.[13−15]

* To whom correspondence should be addressed. E-mail: yanagi@kobe-u.ac.jp.

(1) Tang, C. W.; VanSlyke, S. A. *Appl. Phys. Lett.* **1987**, *51*, 913.
(2) Sheats, J. R.; Antoniadis, H.; Hueschen, M.; Leonard, W.; Miller, J.; Moon, R.; Roitman, D.; Stocking, A. *Science* **1996**, *273*, 884.
(3) Tessler, N. *Adv. Mater.* **1999**, *11*, 363.
(4) Schön, J. H.; Kloc, Ch.; Dodabalapur, A.; Batlogg, B. *Science* **2000**, *289*, 599.
(5) Schön, J. H.; Dodabalapur, A.; Kloc, Ch.; Batlogg, B. *Science* **2000**, *290*, 963.
(6) Tessler, N.; Denton, G. J.; Friend, R. H. *Nature* **1996**, *382*, 695.
(7) McGehee, M. D.; Díaz-García, M. A.; Hide, F.; Gupta, R.; Miller, E. K.; Moses, D.; Heeger, A. J. *Appl. Phys. Lett.* **1998**, *72*, 1536.
(8) Suganuma, N.; Adachi, C.; Koyama, T.; Taniguchi, Y.; Shiraishi, H. *Appl. Phys. Lett.* **1999**, *74*, 1.
(9) Frolov, S. F.; Fujii, A.; Chinn, D.; Vardeny, Z. V.; Yoshino, K.; Gregory, R. V. *Appl. Phys. Lett.* **1998**, *72*, 2811.
(10) Yablonovitch, E. *Phys. Rev. Lett.* **1987**, *58*, 2059.
(11) John, S. *Phys. Rev. Lett.* **1987**, *58*, 2486.
(12) Joannopoulos, J. D.; Villeneuve, P. R.; Fan, S. *Nature* **1997**, *386*, 143.
(13) Grüning, U.; Lehmann, V.; Ottow, S.; Busch, K. *Appl. Phys. Lett.* **1996**, *68*, 747.

10.1021/cm010615a CCC: $20.00
Published on Web 10/05/2001

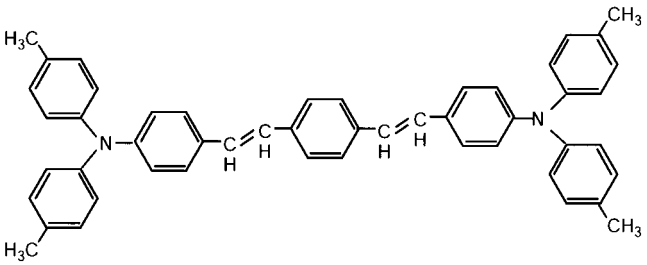

Figure 1. Moleclar structure of DADSB.

However, such techniques are not suitable for application to soft materials composed of organic molecules. Self-organizing processes involving organic molecules is one possible way for mesostructure fabrication.

Recently, we found that organic microdots of fluorescent bis(*N*,*N*-di-*p*-tolylamino-*p*-styryl)benzene (DADSB, Figure 1) molecules were self-organized when vapor-deposited onto the KCl (001) surface.[16] The as-deposited microdots exhibited a bluish green fluorescence, but which considerably quenched under ultraviolet (UV) excitation in air due to photo-oxidation of the π-conjugating distyryl benzene backbone. However, when the microdots were encapsulated in an overcoating MgF_2 layer, this fluorescence quenching was thoroughly prevented. Such stabilized fluorescence is expected to be amplified by self-microcavity effects of the microdots since the emitted light is confined inside them due to a higher refractive index of DADSB than the KCl substrate and MgF_2 layer. In this context, here, we describe their light amplification behaviors under optical pumping excitation.

Experimental Section

Fabrication of microdots was carried out by vapor deposition onto a freshly cleaved (001) surface of a KCl single crystal. Under a vacuum of 5×10^{-4} Pa, the DADSB molecules loaded on a resistively heated quartz crucible were deposited onto the KCl substrate kept at 180 °C. The deposition rate was controlled to give a thickness rate of ≈10 nm/min on a quartz crystal microbalance (QCM) monitor. The morphology of the as-deposited microdots was observed using an atomic force microscope (JEOL JSPM-4200) by the ac mode with a Si cantilever. The microdot specimens were then encapsulated in an MgF_2 layer. After the DADSB microdots were formed on the KCl surface at 180 °C, the substrate was cooled to room temperature and then MgF_2 powder loaded on a coiled tungsten basket was vapor-deposited onto the microdots on KCl. The thickness of the MgF_2 layer was controlled to be ≈1 μm by QCM.

Photoemission experiments of the DADSB microdots were performed under optical pumping using a frequency-tripled Nd:YAG pulse laser (λ_{ex}=355 nm; pulse width, 5 ns; repetition, 10 Hz). The excitation laser was horizontally focused on the sample surface in a line of 1-mm width through a cylindrical lens. The emitted light was collected along the direction parallel to the substrate surface with a CCD spectrometer. The excitation pulse energy was controlled by a 1/2 waveplate and polarizer and was measured with a thermopile sensor.

Results and Discussion

Figures 2a and 2b show representative atomic force microscopy (AFM) images of the microdots grown for 5 and 30 min after starting deposition, respectively. At the initial stage (Figure 2a), AFM profiles of the grown dots show that their diameter and height are around 1 μm and several tens of nanometers, respectively. Some microdots are seen aligning in a line, suggesting that they nucleate along a step of the cleaved KCl surface. In situ optical microscopy revealed their sequential growth process as follows.[16] The microdot nuclei grow larger as the deposition continues. At 10 min after deposition, the number of the microdots was already saturated. Further deposition caused coalescence of the adjacent microdots, resulting in an increase of the diameter and decrease of the number of the microdots. Finally, at a later stage of the growth (Figure 2b), their diameter and height reach larger than 10 and 1 μm, respectively. Such a growth feature as these isolated microdots is based on the "molecular bearing" effect of the bulky peripheral groups in DADSB, which resulted in surface migration of the deposited molecules with long diffusion length. As the DADSB molecules hardly crystallize due to this bulky structure, the grown microdots are found to be amorphous by electron diffraction observation. Figure 3 shows a relation between the diameter and height of the microdots taken at different stages of the growth. At the initial stage of the growth where their diameter was below 5 μm, the diameter and height proportionally increased with a height/diameter ratio of ~1/20. The morphology of the

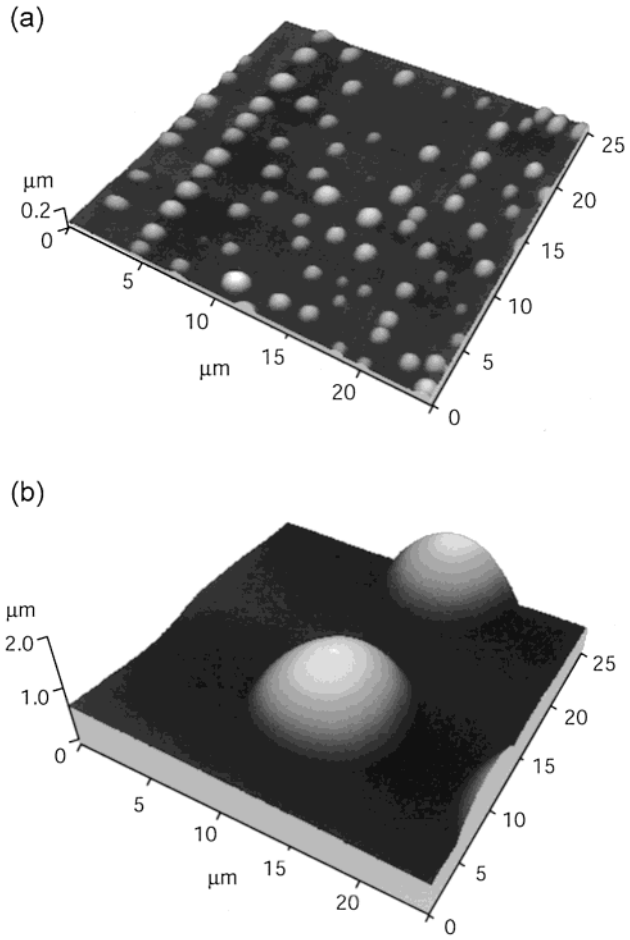

Figure 2. AFM images of DADSB microdots as-deposited on the KCl (001) surface. The images (a) and (b) were taken from microdots grown for 5 and 30 min after starting deposition, respectively.

(14) Kawakami, S. *Electron. Lett.* **1997**, *33*, 1260.
(15) Baba, T.; Matsuzaki, T. *Jpn. J. Appl. Phys.* **1996**, *35*, 1348.
(16) Yanagi, H.; Matsuoka, N.; Kondo, M.; Nagawa, M.; Taniguchi, Y. *Langmuir* **2001**, *17*, 5491.

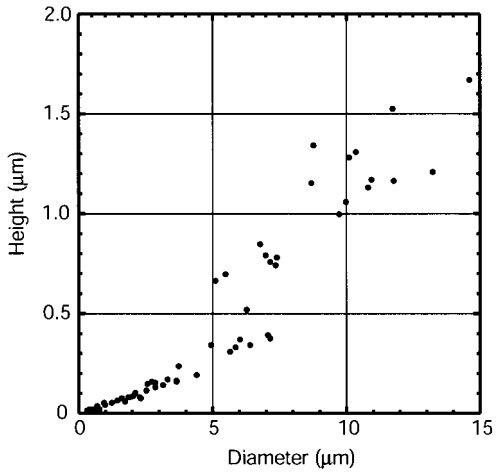

Figure 3. Relation between diameter and height of as-deposited DADSB microdots measured by AFM profiles at various growth stages.

microdots is rather disclike. Further deposition gave rise to an increase of this ratio up to 1/10−1/8, although its distribution became dispersive. This morphological change during the deposition growth can be attributed to interfacial dynamics of the microdots on the KCl surface. At the initial stage of the growth, interaction with the substrate surface tends to make the morphology thinner and disclike. As the microdots grow thicker, their morphology becomes energetically stable with a higher height/diameter ratio.

To prevent photo-oxidative degradation of the DADSB molecule under UV excitation,[16] the as-deposited microdots were encapsulated with an MgF_2 layer. Thus encapsulated microdots exhibited no fluorescence quenching under UV excitation in air; therefore, they were used for the following optical pumping experiments. Figures 4a and 4b show changes of emission spectra with increasing excitation pulse energies for DADSB microdots having average diameters of 7.2 and 13.7 μm (as shown in the inset micrographs), respectively. The smaller microdots (Figure 4a) show a broad emission band, which corresponds to spontaneous fluorescence of the DADSB molecule, even at high excitation energies. This fluorescence intensity increases in proportion to the excitation energy. On the other hand, the bigger microdots (Figure 4b) exhibit a gain-narrowed emission peak. Above a certain threshold energy, the spectral band collapses at the wavelength of the fluorescence maximum (λ = 510 nm). This narrowed peak can be assigned to ASE. Because the refractive index of DADSB measured by ellipsometry is about 2.1 while those of the MgF_2 layer and the KCl substrate are 1.38 and 1.49, respectively, the emitted light of DADSB can be effectively confined inside the microdots. Therefore, the emitted light is amplified at the highest fluorescence efficiency by multiple reflection inside the microdots. This light confinement effect is dependent on the size of the microdots. Figure 5 shows a gain-narrowed peak intensity and line width as a function of pumping pulse energy for DADSB microdots having different diameters. In the case of the microdots with diameters of 6.9 and 7.2 μm, the emission intensity is very low even at high excitation energy. Their bandwidth is almost constant and never collapses. By contrast, the larger microdots with diameters of 9.3 and 13.7 μm show narrowing of the line width above a threshold energy of $\approx$100 μJ/cm^2. These findings suggest that there is a certain cutoff size for gain-narrowing between 7.2 and 9.3 μm in diameter. This cutoff diameter seems reasonable for light confinement. As seen from Figure 3, the height corresponding to those microdots is around 1 μm. Judging from their rounded morphology (Figure 2), the effective height is less than this value, that is, comparable to the wavelengths of the emitted light because the thin edges of the microdots are not responsible for light confinement.

Besides the ASE peak observed for the microdots larger than the cutoff size, periodic sideband modes are sometimes seen at a high pumping energy, as shown in

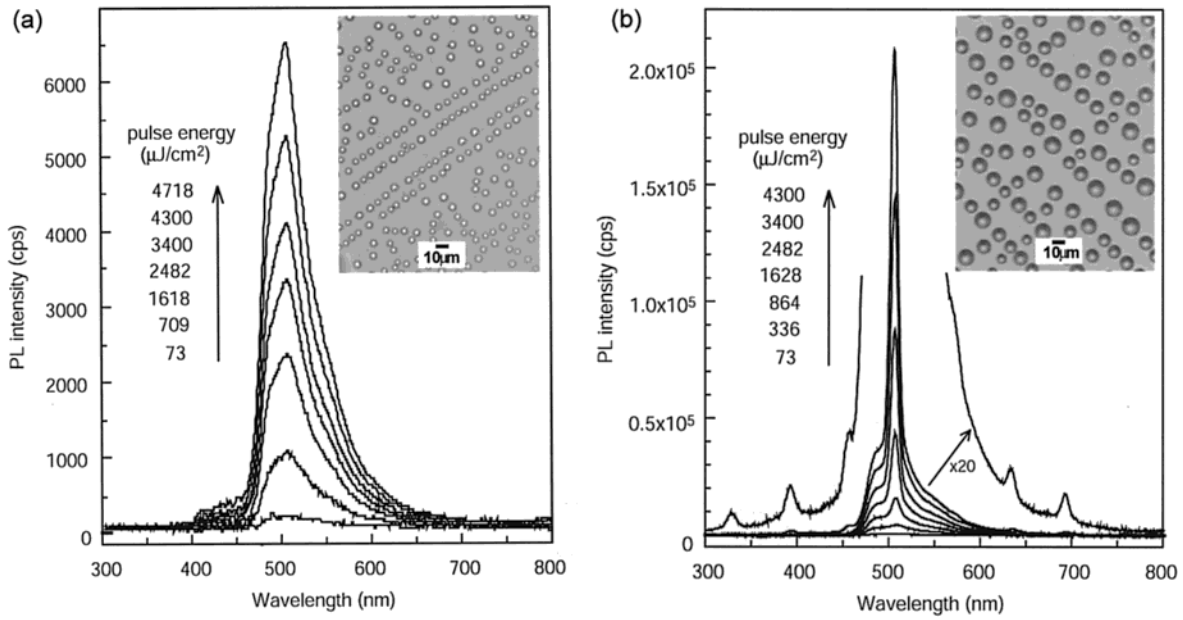

Figure 4. Photoluminescence spectra taken from the DADSB microdots covered with an MgF_2 layer under optical pumping at various excitation pulse energies. Average diameters of the microdots in (a) and (b) are 7.2 and 13.7 μm, respectively, as seen from optical micrographs in the insets.

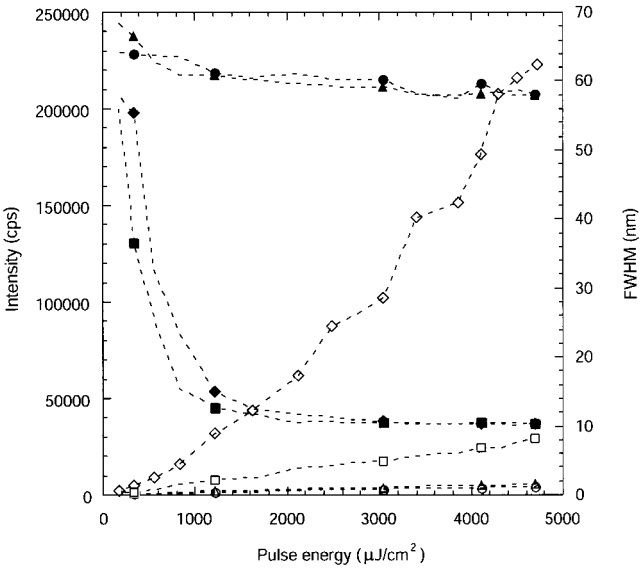

Figure 5. Photoluminescence intensity (open) and line width (solid) of the emission band around $\lambda = 510$ nm as a function of excitation pulse energy for DADSB microdots having average diameters of 6.9 (○, ●), 7.2 (△, ▲), 9.3 (□, ■), and 13.7 μm (◇, ♦).

the enlarged spectrum in Figure 4(b). At first this reminded us that these sidebands could correspond to whispering gallery mode (WGM) lasing. However, a simple calculation based on the WGM resonance along the circumference of the microdots does not agree with the observed intervals between the mode peaks. It probably depends on the shape of the microdot, which is not a perfect disc but actually has a rounded morphology. Although the details of these sideband modes are under investigation, such morphology can give rise to various resonance modes also in the thickness dimension.

The previously reported growth mechanism for the DADSB microdots[16] suggests a possibility of arranging them in a periodic array by forming regular kink sites on the substrate surface, for example, by using an AFM-indentation technique. Such a two-dimensional fluorescent microdot array is interesting for the formation of emissive photonic crystals. Further control of morphology of the individual microdots and regular alignment in a photonic crystal array would enable us to realize WGM lasing, light guiding, improvement of coherence, reduction of laser threshold, and so on. Moreover, also under investigation is the incorporation of suitable electric contacts to these microdots by transferring them onto a conductive electrode surface for development into electrical injection organic lasing.

Acknowledgment. This work was partly supported by the Photonics Materials Program at the Venture Business Laboratory of Kobe University. Financial supports by Toray Science and Technology Grant is also acknowledged.

CM010615A